SUPPLEMENTARY INFORMATION

Ultrasensitive Surface-Enhanced Raman Scattering Detection in Common Fluids

Shikuan Yang, Xianming Dai, Birgitt Boschitsch Stogin, and Tak-Sing Wong**

Department of Mechanical and Nuclear Engineering & Materials Research Institute

The Pennsylvania State University, University Park, PA 16802, USA

*Correspondence and requests for materials should be addressed to: S.Y. (szy2@psu.edu); T.S.W. (tswong@psu.edu)

S1. Materials and Methods

SLIPS preparation. We used two types of structures as SLIPS substrates. (i) Teflon membranes with average pore size of 200 nm and thickness of approximately 70 μm were purchased from Sterlitech Corporation, WA, USA. The as-received Teflon membranes were attached on a flat glass slide or a concave glass bowl. (ii) Microscale silica bowl arrays were created on the substrates from the monolayer colloidal crystal template using the sol-gel method as previously reported (1). The silica bowl arrays were placed inside a vacuum chamber for vapor phase silanization using 0.5 ml heptadecafluoro-1,1,2,2-tetrahydrodecyltrichlorosilane (purchased from Gelest, Inc.) for 12 hr to obtain the hydrophobic modification. Perfluorinated fluids (Dupont Krytox GPL 100) serving as lubricating liquids were then sprayed onto the Teflon membranes or the silica bowl arrays to form an over-coat. The lubricated sample was then spun at 1000 rpm for 1 min to remove the excess lubricants. The silica bowl array-based SLIPS demonstrated similar performance to the Teflon membrane-based SLIPS in SERS sensing applications. Unless otherwise specified, the SLIPSERS platform was developed using Teflon membranes in this work for simplicity.

SUPPLEMENTARY INFORMATION

Preparation of Au nanoparticles. Au nanoparticles with different sizes were prepared according to previous reports (2) with minor modifications. Briefly, 50 ml $HAuCl_4$ solution (0.03 mM) was heated to boiling temperature, and 0.15, 0.2, 0.4, 0.6, and 0.8 ml sodium citrate (3.9 mM) solution was added to generate Au nanoparticles with a mean size of approximately 88, 57, 45, 36, and 24 nm, respectively (Fig. S6a-e). 45 nm Au particles showed the highest SERS signal intensity (Fig. S6g), therefore these particles were chosen for all of the SLIPSERS experiments. The concentration of Au nanoparticles in the solution was determined by calculations as explained later in this discussion. Sodium citrate reduces Au (III) ions to prepare Au nanoparticles according to the following chemical formula: $HOC(COONa)(CH_2COONa)_2 \bullet 2H_2O + 4HAuCl_4 + 3H_2O \rightarrow 3HOOC(COONa) + 4Au + 16HCl$. By having excess sodium citrate, we can reduce all of the Au (III) ions into Au nanoparticles in our fabrication process. Based on the amount of $HAuCl_4$ introduced in the solution, we can calculate the weight of the Au nanoparticles in the solution (~0.3 mg). Note that the weight of a 45 nm Au nanoparticle is ~9.2 x 10^{-13} mg. Considering that the prepared Au nanoparticles have a narrow size distribution with a mean size of 45 nm, the number of Au nanoparticles in the 50 ml Au colloid solution is estimated to be ~3.0 x 10^{11}. Therefore, the molar concentration of the as-prepared Au nanoparticles is determined to be ~ 10 pM. The prepared Au colloidal solution was centrifuged and cleaned three times to remove any unreacted chemicals. The final concentration of the Au colloidal solution was diluted to ~5 pM, which has ~3x10^9 nanoparticles per milliliter (~ 5 pM).

Fabrication of Ag octahedrons. Ag_2O octahedrons were prepared according to previous reports (3, 4) with minor modifications. Ammonia hydroxide solution (1 M) was continuously added

into 5 ml of $AgNO_3$ aqueous solutions (1 M) containing 1 ml of poly(vinyl pyrrolidone) (0.1 mM) until the solution became transparent. Subsequently, 3 ml of NaOH (2 M) solutions were introduced into this colorless solution, yielding black precipitates of Ag_2O octahedrons. The black precipitates were cleaned three times by centrifugation, and then re-dispersed into 10 ml of H_2O_2 solutions (2 M) to reduce the Ag_2O octahedrons into surface roughened Ag octahedrons (Fig. S19).

Black Si preparation. Black Si was prepared using deep reactive ion etching method according to a previous publication (5). The water contact angle on the black Si surface is around 170º with negligible contact angle hysteresis, indicating its superhydrophobicity (Fig. S24).

SERS measurement. SERS measurement was performed on a WITec confocal Raman instrument equipped with a 633 nm wavelength laser. The laser intensity was measured to be ~0.5 mW. The integration time of the SERS signal was 5 s unless otherwise specified. By focusing with a 40× objective, the laser spot size is ~ 1 μm. SERS mapping measurements over an area of 20 μm × 20 μm on the Au aggregate by performing a raster laser scan (Figs. S9-S16) were performed to find observable signals from highly diluted solutions.

Analyte detection on SLIPSERS. Organic or aqueous solutions (50 μl, unless otherwise specified) containing analyte molecules at different concentrations were loaded onto the SLIPSERS platform with a pipette. The SLIPSERS platform was put on a horizontal surface to prevent droplet translation. When a large amount of analyte solution (for example, 1 ml) was used, SLIPSERS was prepared on a concave glass lens. 10 μl of 5 pM Au colloidal solution was

injected into a droplet of the analyte solution and mixed thoroughly. 10 µl of Au colloidal solution was determined to be the best volume for the SLIPSERS platform (Fig. S7). If the amount of the Au nanoparticle is not sufficient (e.g., < 5 µl), then the aggregate formed would be too thin and may experience damage during SERS measurements, giving rise to weak SERS signals (Fig. S7).

Depending on the properties of the solvent and the analytes, solvent evaporation process can be accelerated by heating the solutions at appropriate temperatures (Fig. S21). In our case, 65 ^{o}C heating treatment was used to prevent degradation of the analytes (i.e., biological molecules). After all of the solvent evaporated, the analyte and Au particles formed an aggregate which appeared as a small black dot visible to an unaided eye. SERS measurements were conducted on this aggregate, which consisted of closely packed Au nanoparticles and analyte molecules.

S2. Evaluation of the enrichment efficiency on SLIPSERS platform

To quantify the enrichment efficiency of SLIPSERS, we used copper sulfate solution because it forms a well-defined crystal upon solvent evaporation. 50 µl of copper sulfate solution containing 5 mg of solute was loaded onto SLIPSERS platform. After weighing the copper sulfate crystal formed on the SLIPSERS platform, the enrichment efficiency on the SLIPSERS platform (defined as the mass of analyte in the aggregate divided by mass of analyte in the solution) is estimated to be 97.3 ± 2.4 % based on five independent experiments (Fig. S2). The high analyte enrichment efficiency is attributed to the slippery (i.e., nearly pinning-free) surface of the SLIPSERS platform, where the evaporating droplet can collect almost all the analytes into a single aggregate.

To quantify the detection capabilities of the SLIPSERS platform, we compared its analyte

enrichment performance to that of regular superhydrophobic surface (Teflon nano-porous membrane) using ethanol as a carrier fluid (Fig. S3). We used Rhodamine 6G (R6G) as a test molecule because it readily dissolves in many common solvents. We found that while regular superhydrophobic surfaces formed ring-like stains, our SILPSERS platform was capable of enriching R6G molecules into a single aggregate with near 100% efficiency. Owing to the high solute collection efficiency, R6G molecules enriched from their ethanol solution even at 0.1 nM can be observed by an unaided eye. In comparison, R6G solution with concentrations less than 0.5 μM left no noticeable trace on the superhydrophobic surfaces.

The enhanced analyte collection efficiency of the SLIPSERS platform compared to that of regular superhydrophobic surfaces is attributed to greatly reduced pinning on the SLIPSERS platform. To quantify this observation, 10 μl water and ethanol droplets containing 0.17 wt.% polystyrene (PS) beads (1 μm in size) were allowed to evaporate on superhydrophobic surfaces (Teflon nano-porous membranes) and SLIPS. Side-view images of the evaporating droplets were captured by a contact angle goniometer (ramé-hart model 295) at set time intervals (60 s for water, 10 s for ethanol) until the droplet completely evaporated. The images were then analyzed using home-built MATLAB software that detected the contact length of the droplets for each image. The data were subsequently converted into plots depicting droplet contact length versus time (Figure S1). The contact length, L, of each droplet were normalized by the droplet's original contact length, L_0. Time, t, was normalized by amount of time it took the individual 10 μl droplet to evaporate, τ. We define dimensionless time to be t^*, such that $t^* = t/\tau$. We observed that both water and ethanol droplets evaporated in a constant contact angle mode on SLIPS without noticeable pinning at the contact line, until the particles clustered together to form a three-dimensional aggregate. This mode of evaporation is consistent for various aqueous and

non-aqueous colloidal solutions (i.e., toluene, methanol, acetone, and dichloromethane). For the superhydrophobic surface, the ethanol droplet evaporated in a constant diameter mode, indicating significant pinning at the contact line (Fig. S1).

Our studies demonstrate that our SLIPSERS platform can enrich objects with sizes ranging from sub-nanometer (e.g., small molecules and ions) to nanometer (e.g., colloids, Fig. S5) to micrometer (e.g., PS beads, Fig. S1 and Fig. 1B in the main text) dispersed in almost any liquids. To our knowledge, it is the only platform that can achieve complete particulate collection in commonly used liquids, and can therefore substantially improve SERS analysis.

S3. Advantage of SLIPSERS platform over traditional SERS substrates

Superhydrophobic surfaces can be used as an analyte concentrator in aqueous phase detection. However, in real samples, analytes are usually dispersed in different phases including air, organic liquids and water. As an analyte concentrator, superhydrophobic surfaces cannot be used for organic and biological fluids. Even in aqueous phase detections, superhydrophobic surfaces suffer from several serious issues. First, Cassie-Wenzel transition will take place when the evaporating drop is small (6), which results in reduction of analyte enrichment efficiency (Figs. S24 and S25). Second, the aqueous analyte solution on the superhydrophobic surface could take a substantial amount of time to fully evaporate. For instance, it takes more than 4 hr for a 60 μl of water droplet to fully evaporate on the superhydrophobic black Si surface under ambient conditions. Elevating the temperature or lowering the pressure could speed up the evaporation process, but both techniques make the droplet more likely to enter the “sticky” Wenzel state, thus greatly reducing the analyte enrichment efficiency due to droplet pinning (Fig. S26).

SLIPSERS is an ideal platform for concentrating and delivering analyte molecules to SERS

hot spots. Moreover, it is effective in detecting analytes not only in water but also in commonly used organic and biological liquids. The SLIPSERS platform can withstand temperatures >100 ºC, substantially accelerating the solvent evaporation process (*e.g.*, <5 min, Figure S21), while maintaining a high analyte collection efficiency (~98%). Furthermore, ions, molecules, nanoparticles, and colloids with sizes ranging from sub-nanometer to micrometer can all be enriched on the SLIPSERS platform, forming a three-dimensional particle/analyte aggregate upon solvent evaporation.

Most notably, analytes can be enriched and delivered into the Au aggregate that are independent of the interactions with the Au nanoparticles. Therefore, any SERS-active analytes can be detected using the SLIPSERS system. The small crevices between adjacent Au nanoparticles in the aggregate serve as SERS hot spots (Fig. S8). Hence, ultrasensitive detection of analyte molecules in aqueous, organic and biological liquids at femtomolar concentration or below could be achieved with good reproducibility using our SLIPSERS system. Therefore, our system may extend the capability of SERS to other fields such as organic chemistry and life sciences (e.g., for the detection of extremely low concentrations of biomarkers in complex biological fluids).

S4. Finite-difference time-domain (FDTD) simulation of electric-field distribution

To understand the mechanism of SLIPSERS and to simulate the optical field distribution on the three-dimensional Au nanoparticle aggregate, a computer simulation was performed using FDTD method (Lumerical, Inc., Canada). The optical field enhancement on a 5×5×5 array of close-packed 45 nm Au nanoparticles was simulated (Fig. S8). The incident light was a plane wave propagating from the top to the bottom of the nanoparticle array. The monitor was placed at the

bottom of the nanoparticle array facing the light source. The polarization of the 633 nm laser is shown in Fig. S8. Parameters used in the FDTD simulation for Au nanoparticles are supplied by the software without modifications. In our simulation, a strong optical field is formed between junctions of adjacent Au nanoparticles in the top layer. The optical field is slightly weakened in the bottom (fifth) layer of the Au nanoparticles.

S5. Sensitive soil contamination monitoring enabled by SLIPSERS

Standard dust representing soil was purchased from Powder Technology Inc. (Burnsville, USA) with a mean size of 20 μm. The dust (0.5 g) is first contaminated with PCB 7, PCB 77, and PCB 209 at a contamination level of one part per billion (ppb, 10^{-9}). To extract these PCB contaminants, 0.1 g of contaminated soil was suspended into 2 ml of water and acetone, respectively. Next, after the soil precipitates, 50 μl of the water and acetone supernatants with the released PCB contaminants were respectively loaded onto the SLIPSERS platform for analyte concentration and SERS detection. The estimated molar concentration of PCB 7, PCB 77 and PCB 209 are ~0.23, ~0.17 and ~0.1 nM, respectively, assuming that all of the PCB molecules were released into the liquid. However, the actual concentration of PCBs in the solution may be much lower due to the incomplete dissolution of PCBs from the soil particles and the adherence of the molecules to the inner surface of glass container.

Strong SERS signals of PCB can be obtained from the contaminated soil sample dispersed in acetone; no observable signals were detected from the one dispersed in water (Fig. S29). Therefore, appropriate choice of solvent is critical for the successful PCB extraction.

To further demonstrate the detection versatility of the SLIPSERS system in soil contamination detection, we have further studied multiplex detection of PCB 7, PCB 77, and PCB 209 released

from the contaminated soil. To start, 0.1 g of PCB 7, PCB 77, and PCB 209 contaminated soil samples were mixed together before releasing them into 2 ml of water and acetone, respectively. After the soil particles precipitated, 50 µl of the supernatant were extracted from each of the solvents, and loaded onto the SLIPSERS for analyte concentration and SERS detection. SERS signals of PCB 7, PCB 77, and PCB 209 appeared in the samples using acetone as a solvent, while no signals were observed from those of contaminant released in water. Since PCB 7, PCB 77, and PCB 209 molecules are structurally similar, some of their Raman peaks overlapped. The individual signals can be decoupled using a Gaussian deconvolution method (Fig. S30). These experiments further highlight the capability of SLIPSERS for ultrasensitive and multiplex detection in organic liquids.

SUPPLEMENTARY INFORMATION

Supporting Table and Figures:

Table S1. State-of-the-art SERS detection on different engineered substrates.

SERS Substrate	Solution Type	Detection Time	Detection Limit (R6G)
Micro/nanostructured surfaces (7,8)	Water and Organic	~ 30 min	~ 1 pM
Superhydrophobic surfaces (9)	Water	~ hour	10 aM
Nanoparticle film or nanoparticle clusters (10, 11)	Water and Organic	~ hour	~ 1 nM
SLIPSERS	Water and Organic	~ 5 min	~ 1 aM

SUPPLEMENTARY INFORMATION

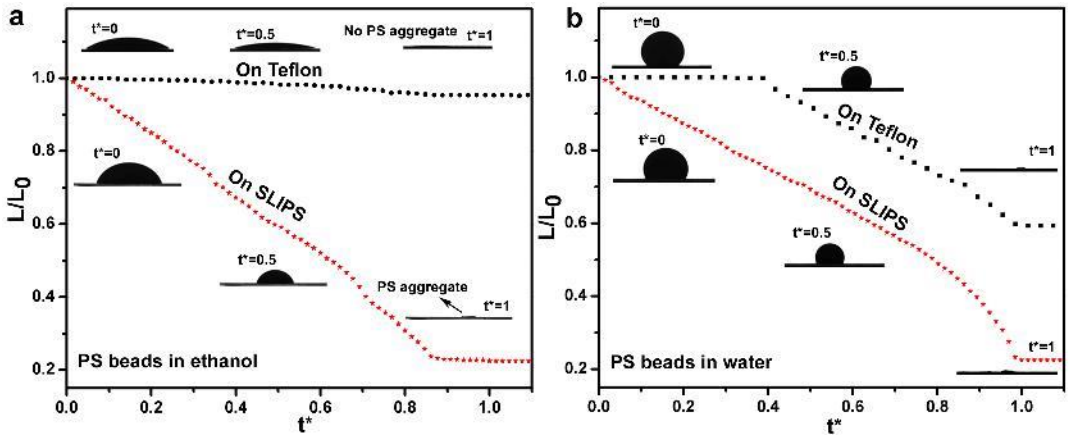

Figure S1. Time evolution of contact length of evaporating droplets on superhydrophobic surfaces and SLIPS. **a,** A 10 µl ethanol droplet containing 0.17 wt.% polystyrene beads evaporating on a superhydrophobic (Teflon) surface and a SLIPS substrate. **b**, A 10 µl water droplet containing 0.17 wt.% polystyrene beads evaporating on superhydrophobic surface and on SLIPS.

SUPPLEMENTARY INFORMATION

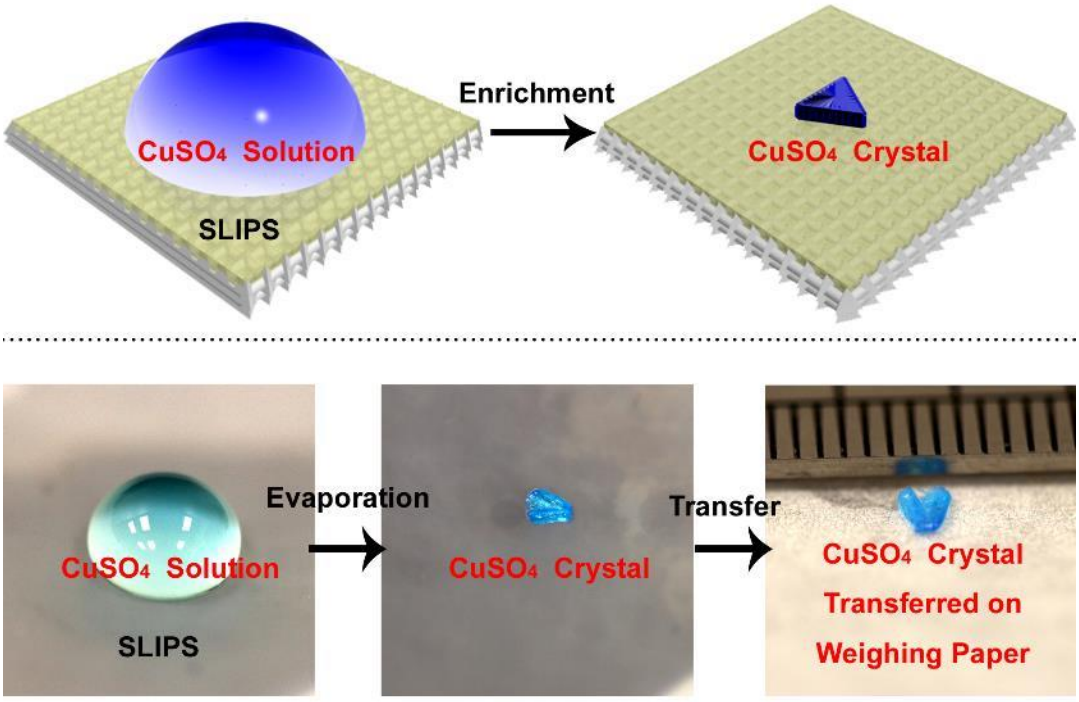

Figure S2. Determination of the enrichment efficiency on SLIPSERS platform. Copper sulfate aqueous solutions are used since the copper sulfate crystal can be easily transferred and weighed. The enrichment efficiency is estimated to be 97.3 ± 2.4 %. The standard deviation is calculated based on five independent measurements.

SUPPLEMENTARY INFORMATION

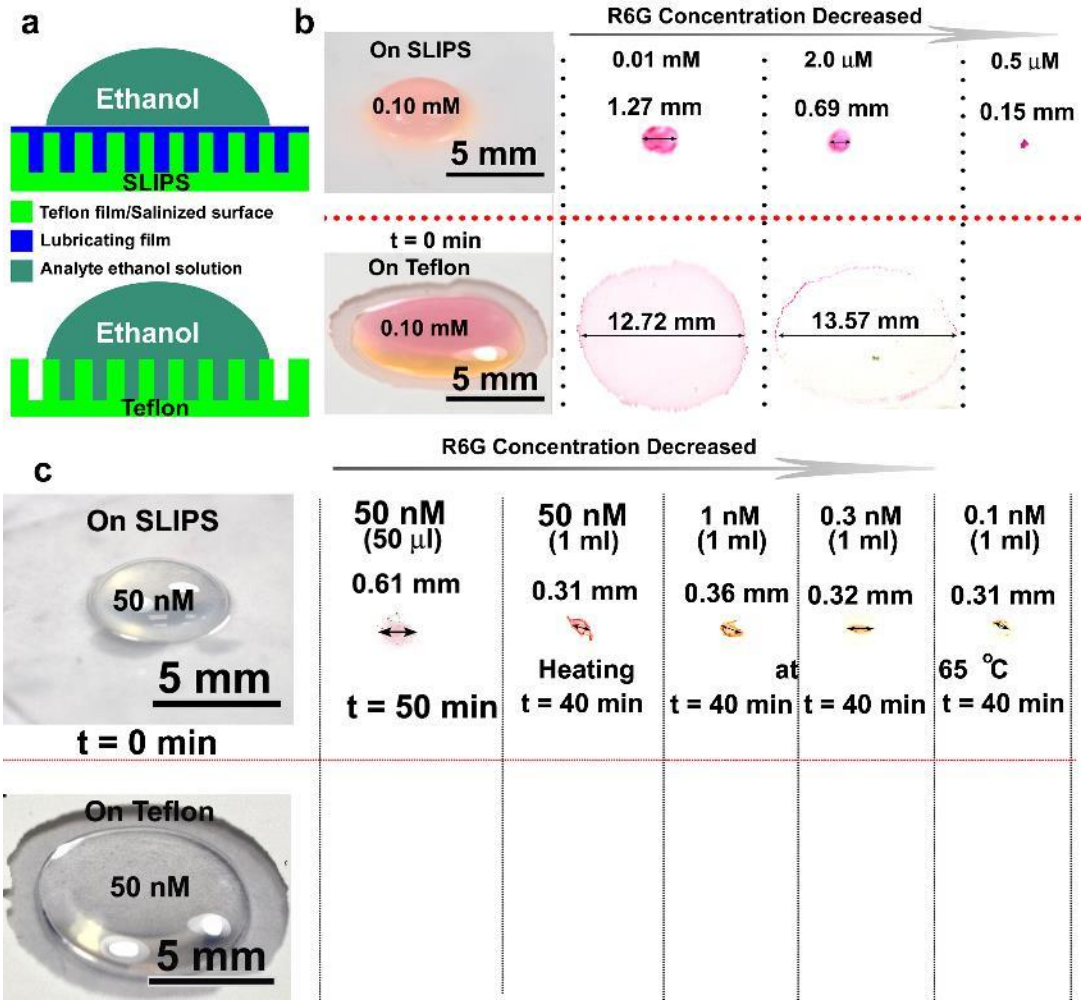

Figure S3. R6G molecules extracted from their ethanol solutions at different concentrations on SLIPS and a superhydrophobic surface (Teflon membrane). **a,** Schematic demonstration of the wetting state of the analyte solution on SLIPS and superhydrophobic Teflon surface. **b,** A tiny R6G aggregate formed on SLIPS. Coffee ring pattern formed on the superhydrophobic Teflon surface when the concentration is higher than ~ 1 μM. No observable solute formed on the Teflon surface when the concentration is lower than 0.5 μM. **c,** Observable aggregates were formed on SLIPS at concentration down to 0.1 nM.

SUPPLEMENTARY INFORMATION

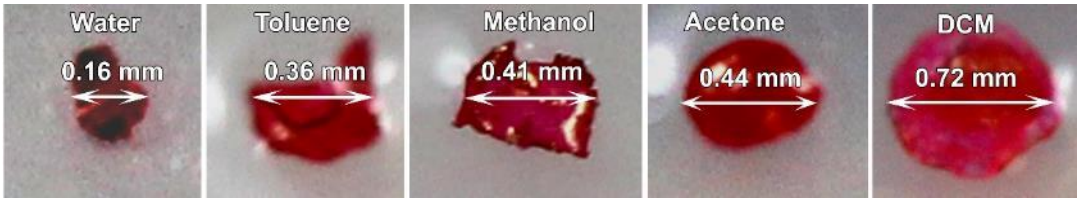

Figure S4. Enrichment of R6G molecules dissolved in commonly used solvents (50 µl) at 1 µM concentration, including water, toluene, methanol, acetone, and dichloromethane (DCM).

SUPPLEMENTARY INFORMATION

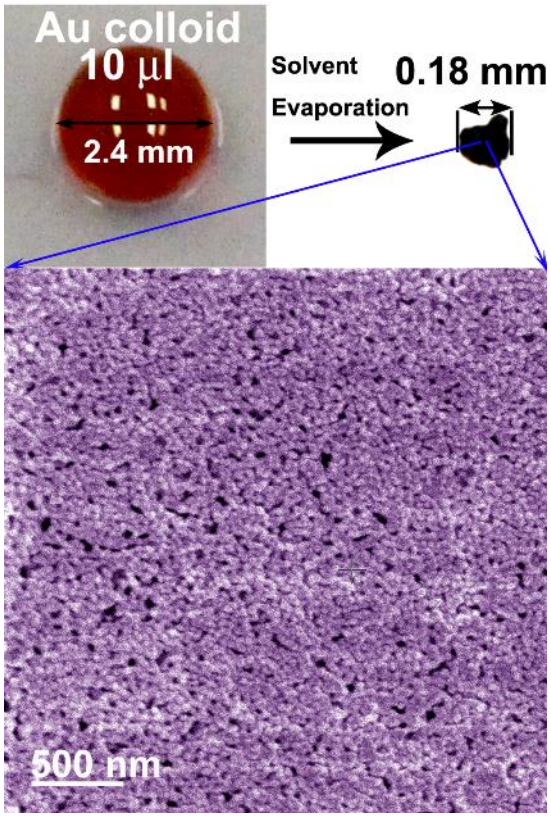

Figure S5. Enrichment of Au nanoparticles in their colloidal solution at 60 ºC on SLIPS. The SEM image shows that these Au nanoparticles are closely packed after water completely evaporated.

SUPPLEMENTARY INFORMATION

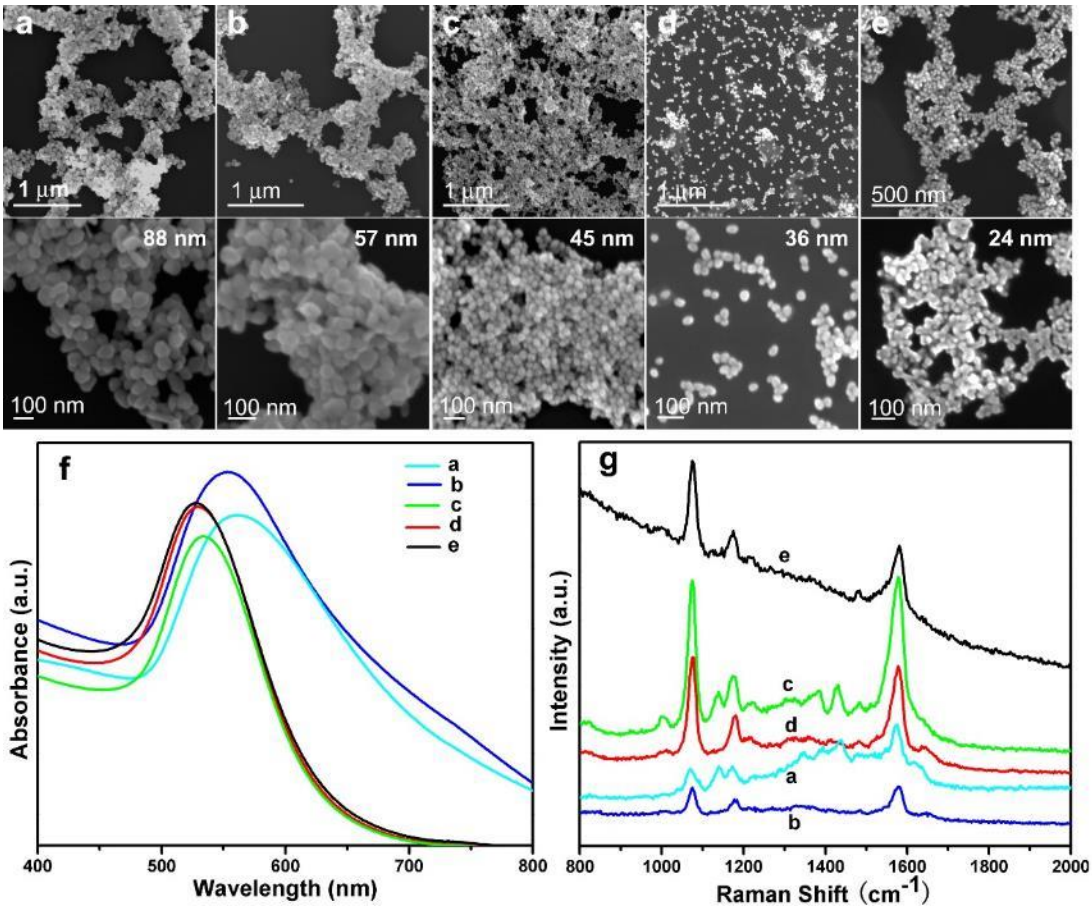

Figure S6. Characterization of Au colloids. a-e, SEM images of the Au nanoparticles with different sizes (sizes depicted in top right corners of the lower panel images). **f**, UV-vis absorption spectra of the prepared Au nanoparticles. **g**, SERS spectra captured from 4-ATP/Au aggregate concentrated from 50 μl 4-ATP ethanol solution (1 nM) and 10 μl Au colloid composed of (a) 88 nm, (b) 57 nm, (c) 45 nm, (d) 36 nm, and (e) 24 nm Au nanoparticles. The SERS integration time was 1 s.

SUPPLEMENTARY INFORMATION

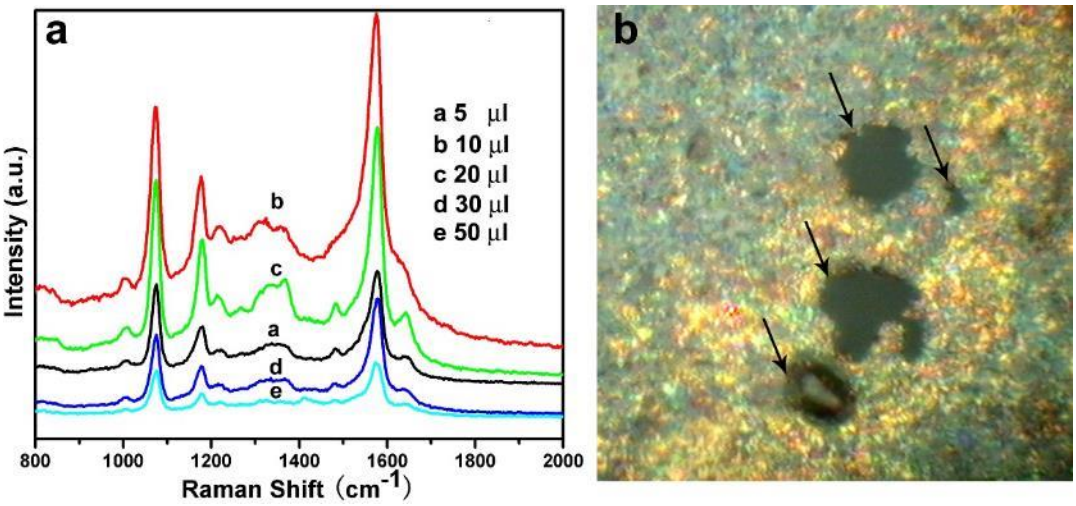

Figure S7. Determination of the best volume of Au colloidal solution needed for SLIPSERS. a, SERS spectra from 4-ATP/Au aggregate concentrated from 50 μl 4-ATP ethanol solution (1 nM) and different amounts of Au colloid are measured. 10 μl is determined to be the best volume. **b,** Damages of an Au nanoparticle aggregate formed from a small volume of Au colloid (i.e., < 5 μl) during SERS measurements.

SUPPLEMENTARY INFORMATION

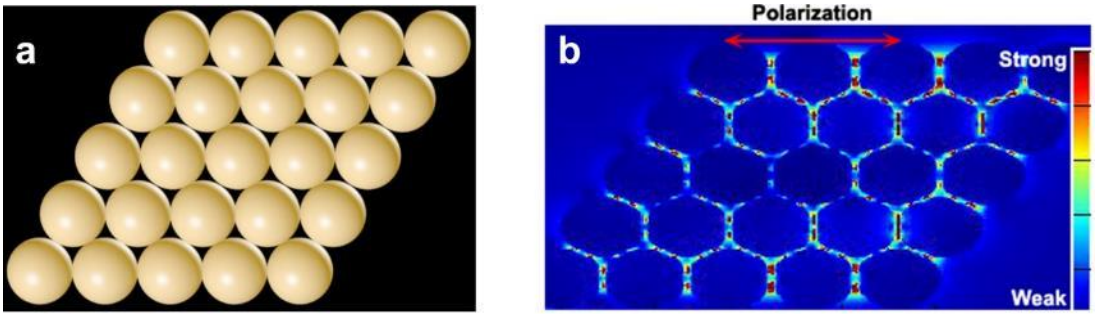

Figure S8. FDTD simulation of the optical field enhancement. a, Simulation model used is a 5×5×5 array of closely packed 45 nm Au nanoparticles. **b,** Top-view of the optical field distribution over the Au nanoparticle array. The polarization of laser signal (wavelength = 633 nm) is shown in b.

SUPPLEMENTARY INFORMATION

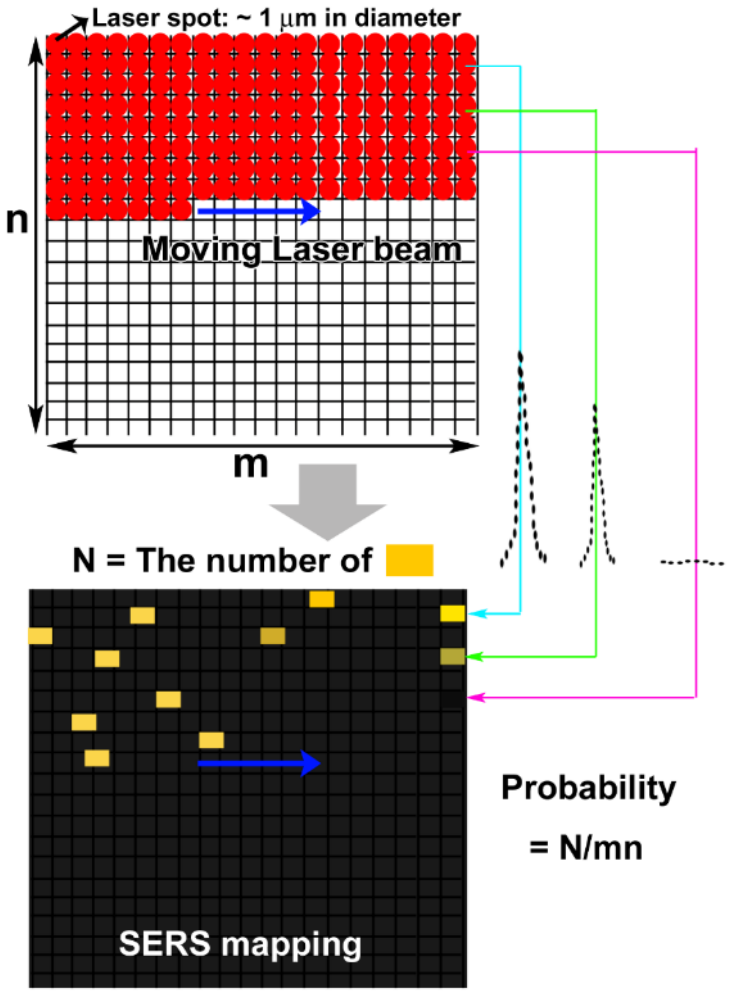

Figure S9. Schematic showing SERS mapping measurement procedures.

SUPPLEMENTARY INFORMATION

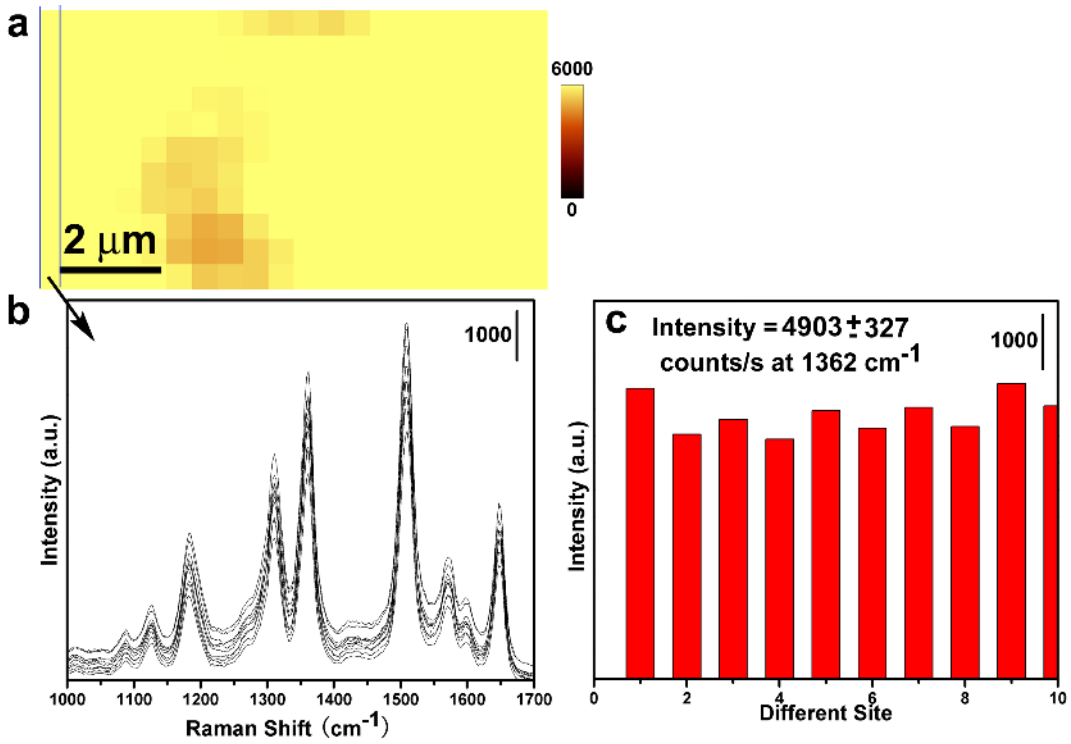

Figure S10. a, SERS mapping result of R6G at 1362 cm^{-1} extracted from 750 nM ethanol solutions. **b,** SERS spectra obtained from the left column in the mapping data. **c,** Raman signal intensity at 1362 cm^{-1} in the SERS spectra shown in b.

SUPPLEMENTARY INFORMATION

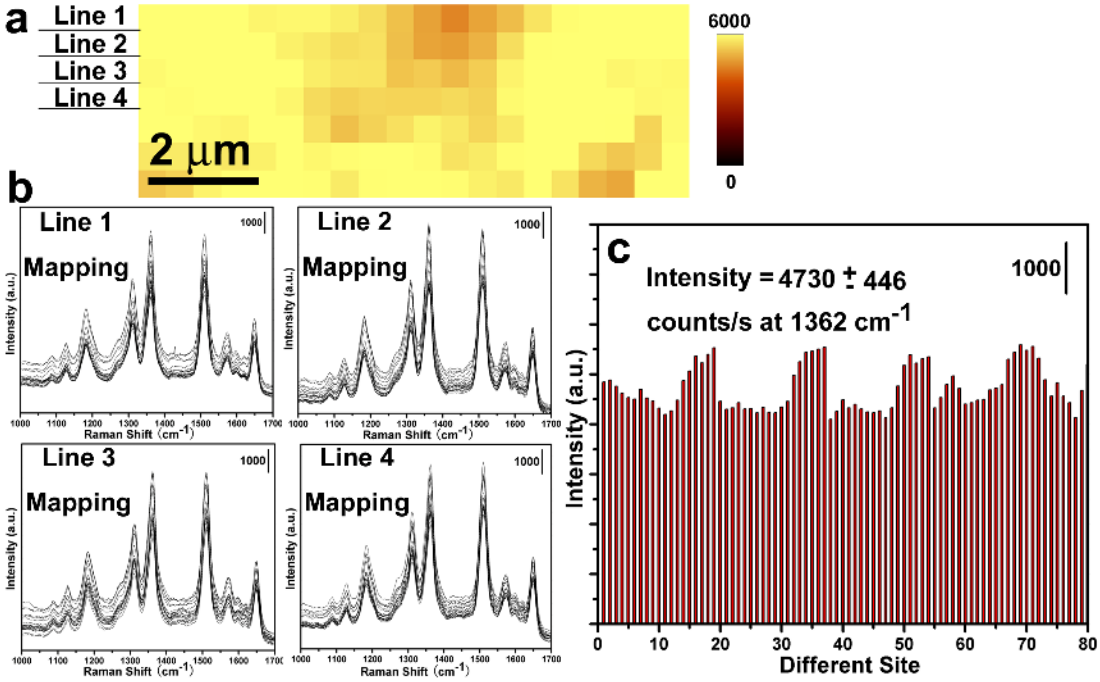

Figure S11. a, SERS mapping result of R6G at 1362 cm^{-1} extracted from 75 nM ethanol solutions. **b,** SERS spectra obtained from the mapping data. **c,** Raman signal intensity at 1362 cm^{-1} in the SERS spectra shown in b.

SUPPLEMENTARY INFORMATION

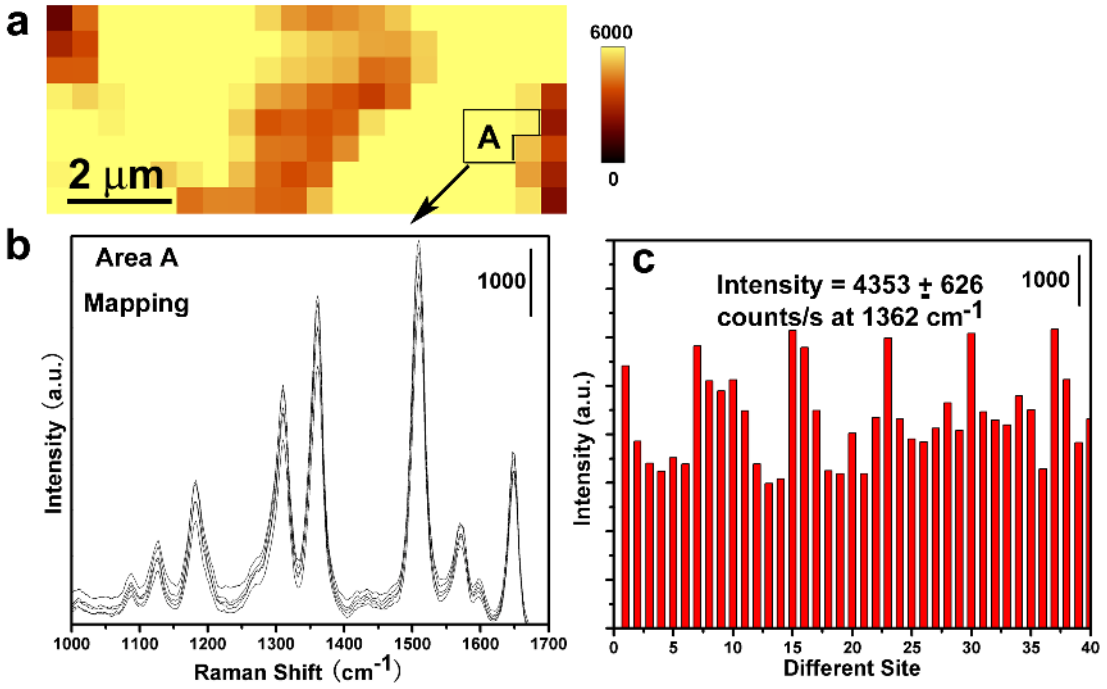

Figure S12. a, SERS mapping result of R6G at 1362 cm^{-1} extracted from 75 pM ethanol solutions. **b,** SERS spectra obtained from area A in the mapping data. **c,** Raman signal intensity at 1362 cm^{-1}.

SUPPLEMENTARY INFORMATION

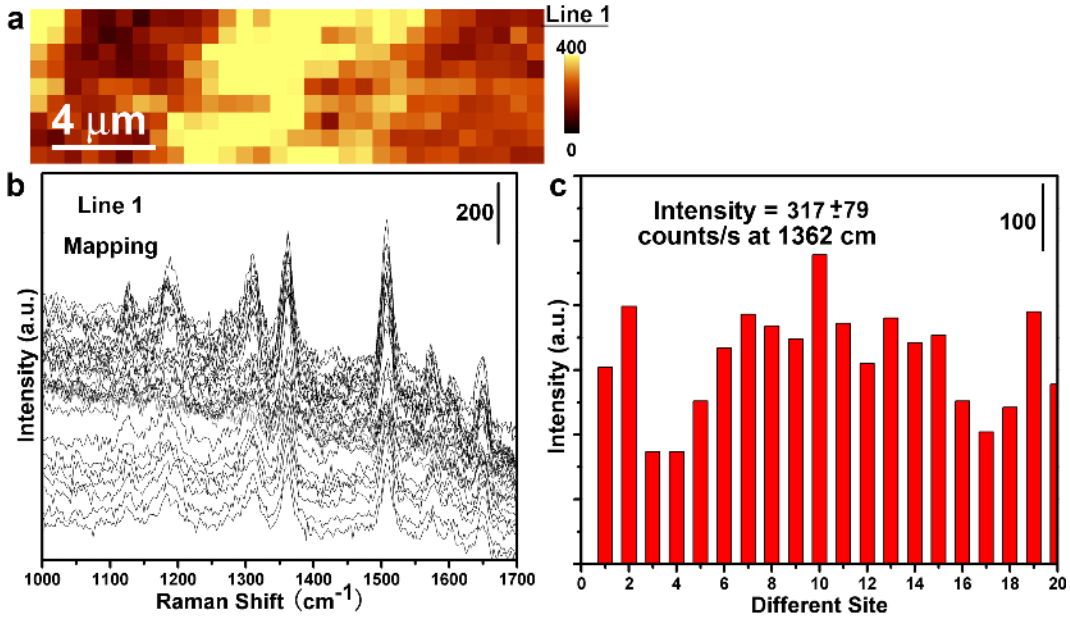

Figure S13. a, SERS mapping result of R6G at 1362 cm^{-1} extracted from 750 fM ethanol solutions. **b,** SERS spectra obtained from Line 1 in the mapping data. **c,** Raman signal intensity at 1362 cm^{-1}.

SUPPLEMENTARY INFORMATION

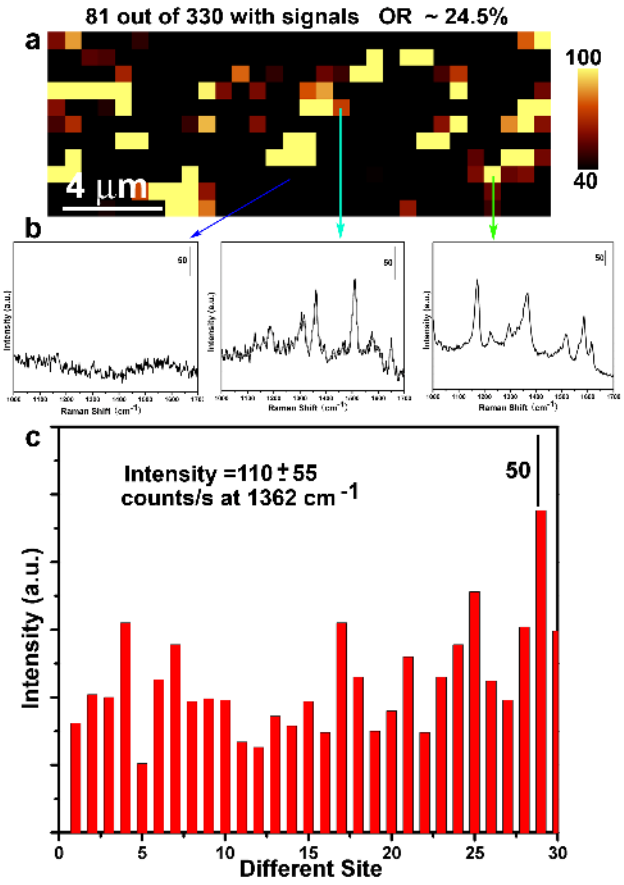

Figure S14. a, SERS mapping result of R6G at 1362 cm^{-1} extracted from 75 fM ethanol solutions. **b,** SERS spectra obtained from marked sites in the mapping data. **c,** Raman signal intensity at 1362 cm^{-1}.

SUPPLEMENTARY INFORMATION

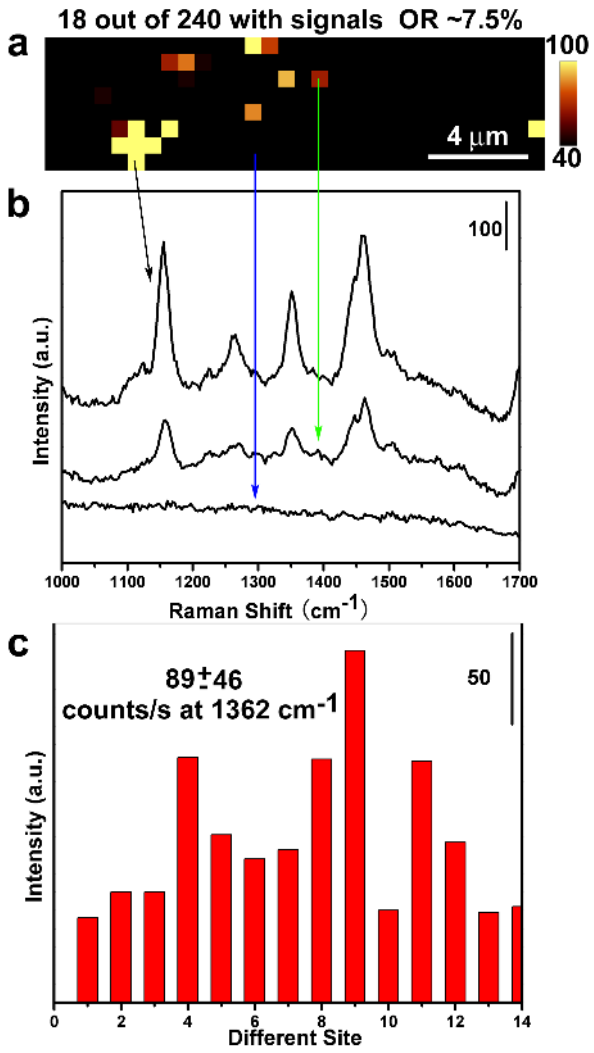

Figure S15. a, SERS mapping result of R6G at 1362 cm^{-1} extracted from 25 fM ethanol solutions. **b,** SERS spectra obtained from marked sites in the mapping data. **c,** Raman signal intensity at 1362 cm^{-1}.

SUPPLEMENTARY INFORMATION

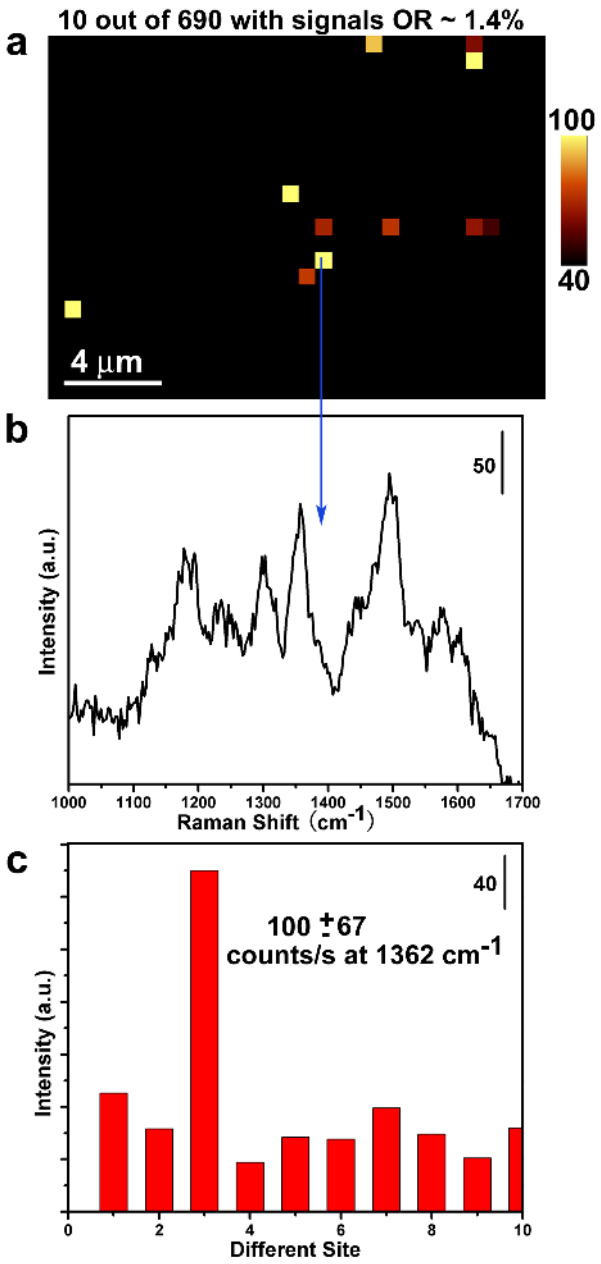

Figure S16. a, SERS mapping result of R6G at 1362 cm^{-1} extracted from 75 aM ethanol solutions. **b,** SERS spectra obtained from the marked site in the mapping data. **c,** Raman signal intensity at 1362 cm^{-1}.

SUPPLEMENTARY INFORMATION

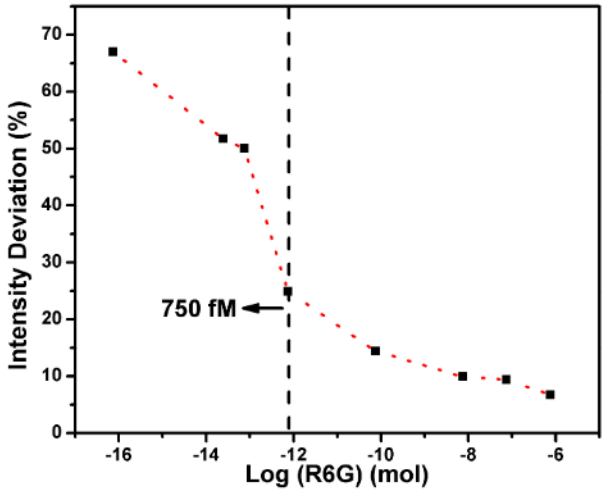

Figure S17. Standard deviations of SERS intensities at 1362 cm^{-1} of R6G at different concentrations. The standard deviations were obtained from more than 20 independent SERS spectra.

SUPPLEMENTARY INFORMATION

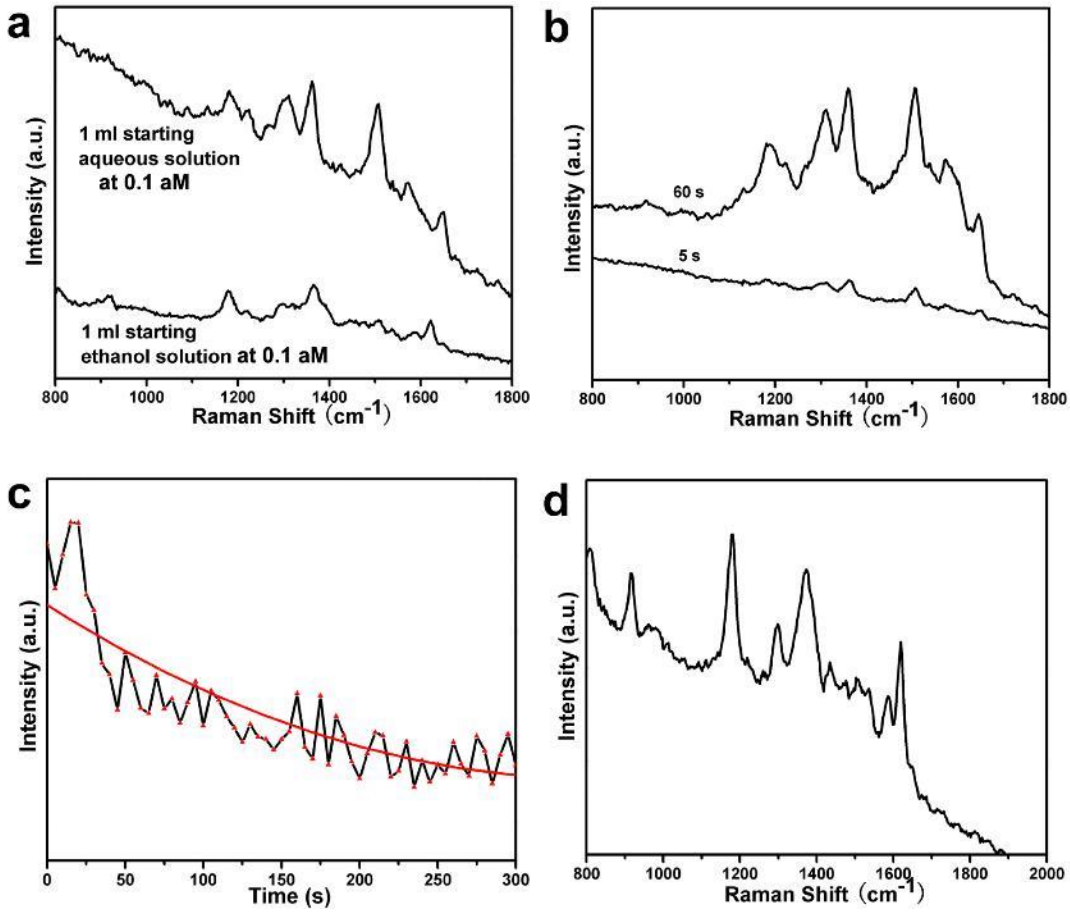

Figure S18. Improvement of the limit of detection of SLIPSERS. a, By using 1 ml solution, the limit of detection can reach 0.1 aM in both water and ethanol. **b,** The SERS signals can be greatly increased by prolonging the integration time. The concentration of the R6G aqueous solution is 10 aM. **c,** The intensity of SERS signal at 1362 cm^{-1} gradually decreases as laser irradiation continues. This indicates that the intensity of the SERS signal cannot be enhanced indefinitely by prolonging the integration time. The starting concentration of the R6G aqueous solution is 1 aM. **d,** Occasionally, strong SERS signals can be observed even at 1 aM concentration.

SUPPLEMENTARY INFORMATION

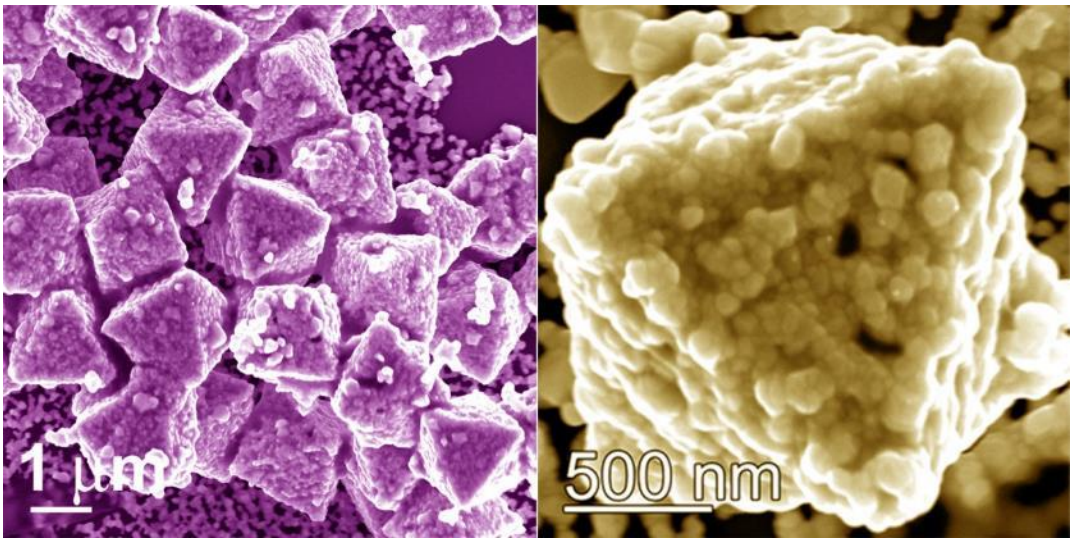

Figure S19. SEM images of Ag octahedrons at different magnifications.

SUPPLEMENTARY INFORMATION

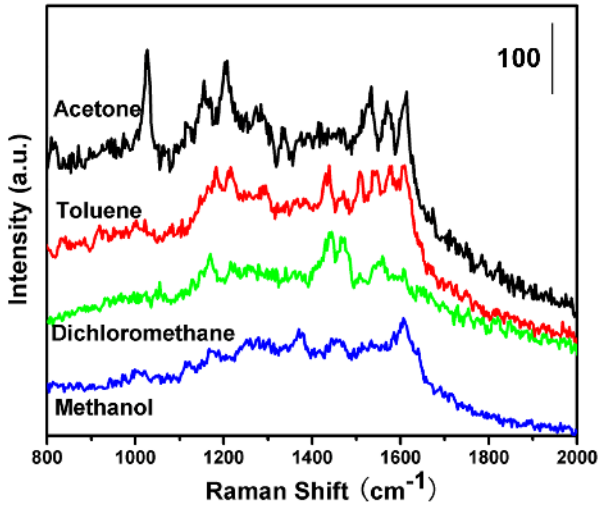

Figure S20. Ultrasensitive SERS detection of R6G molecules dissolved in various organic liquids including acetone, toluene, dichloromethane, and methanol at 1 fM concentration.

SUPPLEMENTARY INFORMATION

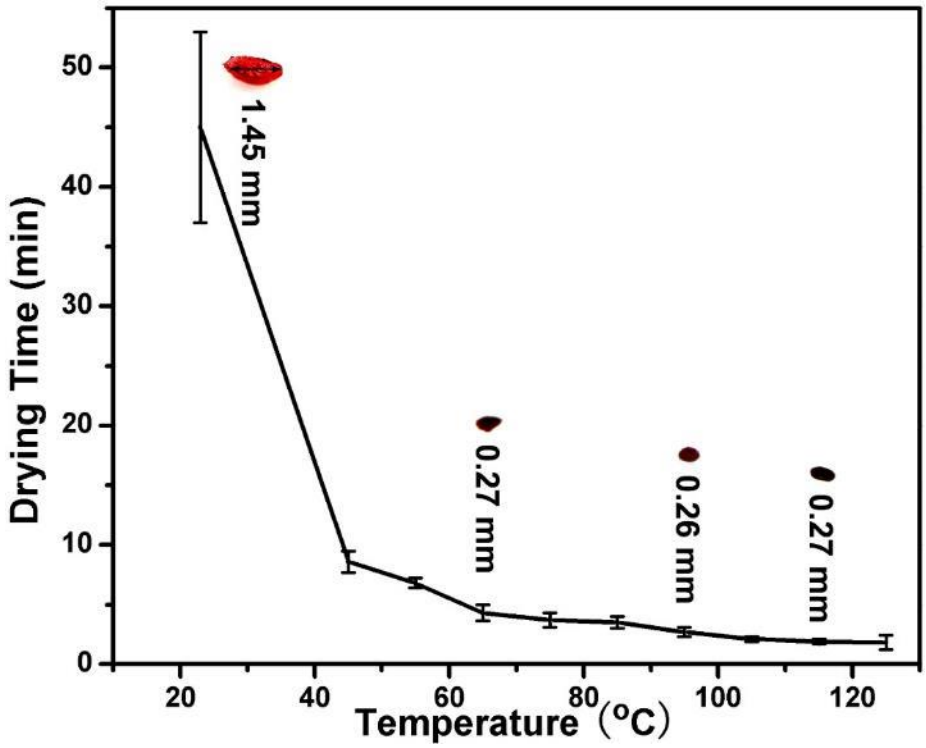

Figure S21. Accelerated enrichment process of R6G molecules in 50 µl ethanol solutions (0.1 mM) at elevated temperatures. The R6G Au nanoparticles aggregate becomes smaller in lateral dimensions but thicker at higher temperatures. The error bars indicate standard deviations from five independent measurements.

SUPPLEMENTARY INFORMATION

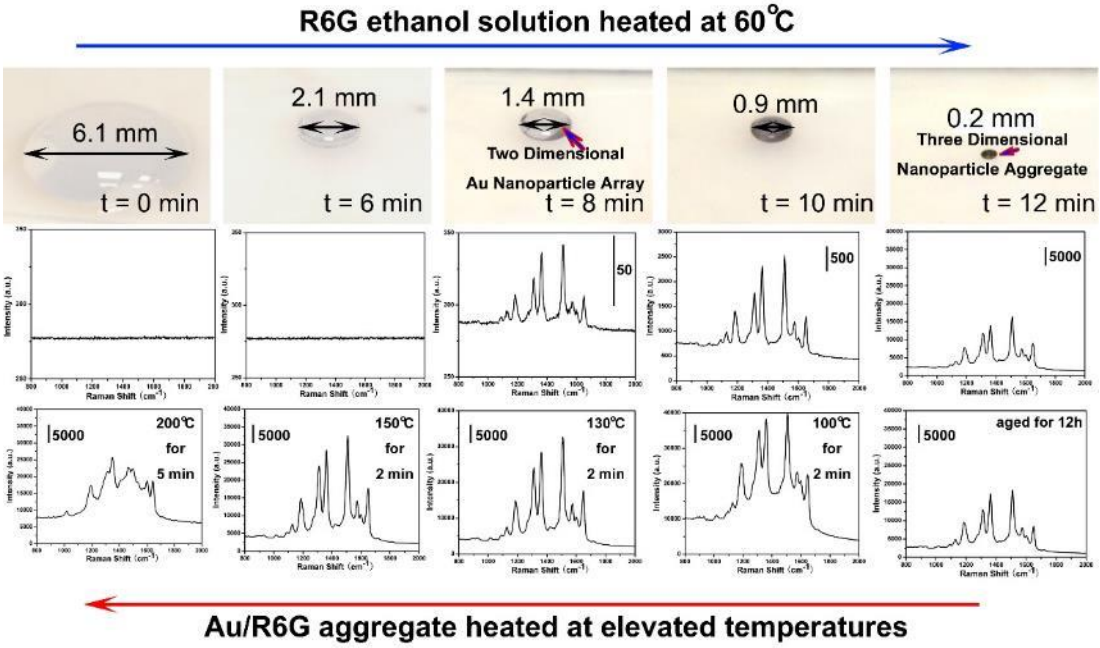

Figure S22. In situ measurement of SERS as the enrichment process proceeds. R6G ethanol solutions (50 µl) at 0.1 µM concentration mixed with 10 µl Au colloidal solution are placed on the SLIPS. After 8 min of solvent evaporation, SERS signals coming from R6G molecules are observable after focusing on the two-dimensional Au nanoparticle array formed on the liquid surface. When the three dimensional Au nanoparticle array formed after 12 min of enrichment, the intensity of the SERS signal increased by more than 200 times. Further heating the R6G/Au nanoparticle aggregate will slightly increase the SERS intensity. The structure of R6G molecules might be deteriorated at very high heating temperatures (e.g., 200 ^{o}C) as reflected from the distorted Raman signals, resulting in reduced SERS signals.

SUPPLEMENTARY INFORMATION

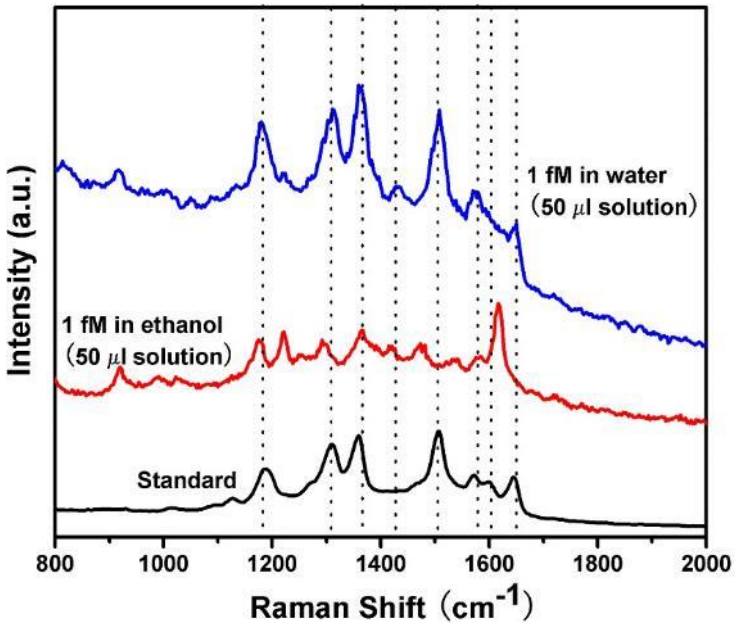

Figure S23. Comparison of Raman peaks of R6G dissolved in different solvents at femtomolar concentrations. The dotted lines are typical locations of R6G Raman peaks. Some vibrational modes shifted slightly when the concentration of the solution is very low, a phenomenon that is frequently observed in single-molecule detections. The electromagnetic field gradient can even induce the appearance of new SERS peaks that are not typically shown in a normal Raman spectrum (12).

SUPPLEMENTARY INFORMATION

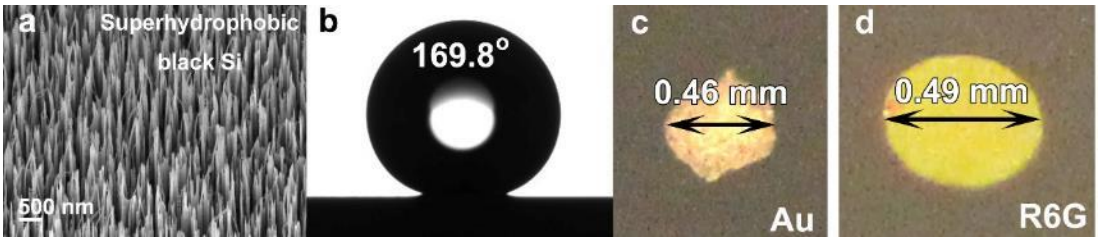

Figure S24. Analyte enrichment on superhydrophobic black Si surface. a, SEM image of the black Si surface. **b,** Water contact angle on superhydrophobic Si surface. **c,** Au nanoparticle aggregate. **d,** R6G solute enriched from 10 µl Au colloidal solution and 50 µl R6G aqueous solution each at 1 µM concentration, respectively.

SUPPLEMENTARY INFORMATION

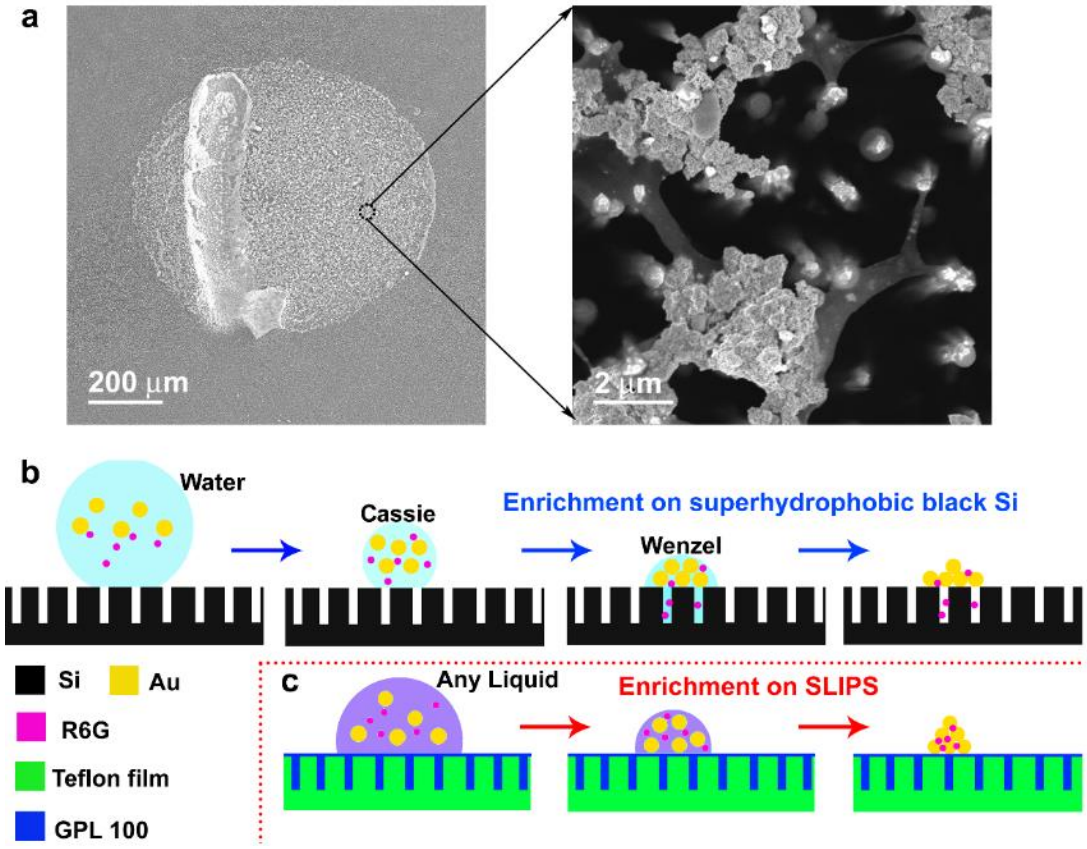

Figure S25. Enrichment process on superhydrophobic surfaces and SLIPS. a, SEM image of Au nanoparticle aggregate on black silicon, showing many Au nanoparticle clusters residing on the tip of Si nanowires. **b, c,** Schematic illustration of the enrichment process on superhydrophobic surface and SLIPS, respectively.

SUPPLEMENTARY INFORMATION

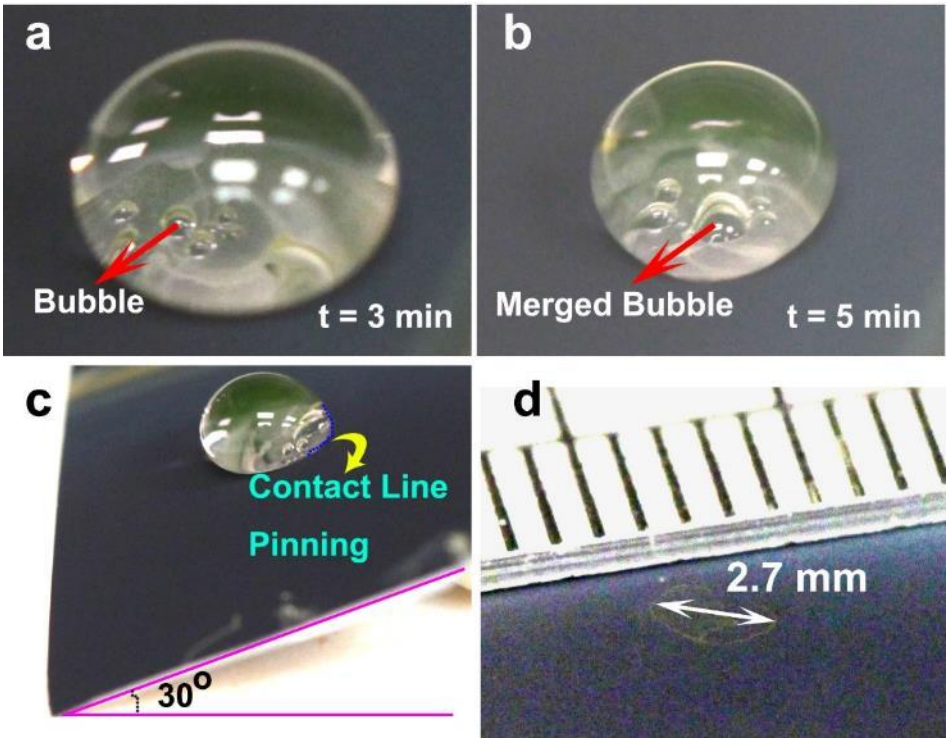

Figure S26. Influence of heat treatment on the enrichment process on superhydrophobic black Si. a, After heating 10 µl of Au colloidal solution at 65ºC for 3 min, small bubbles emerge at the liquid/solid interface. **b,** These bubbles grow rapidly as heating proceeds. **c,** The droplet becomes pinned on the black Si after heat treatment, leading to irreversible Cassie-to-Wenzel transition. **d,** Au nanoparticles spread over a large area, showing poor analyte enrichment during heating on superhydrophobic surfaces.

SUPPLEMENTARY INFORMATION

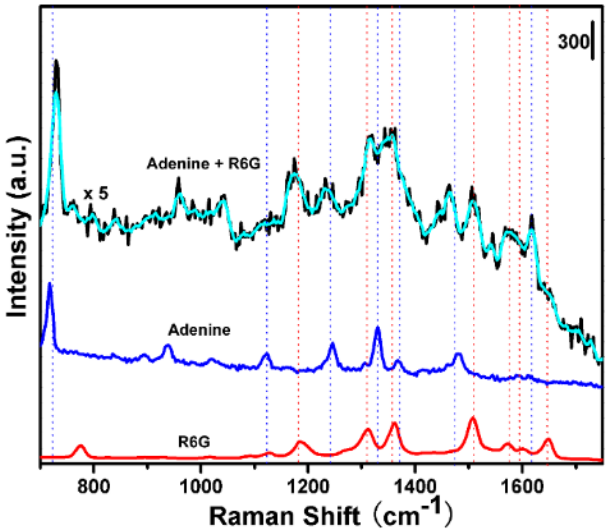

Figure S27. Multiplex and multiphase SERS analysis of R6G (75 fM in ethanol) and adenine (37 fM in water) using SLIPSERS platform.

SUPPLEMENTARY INFORMATION

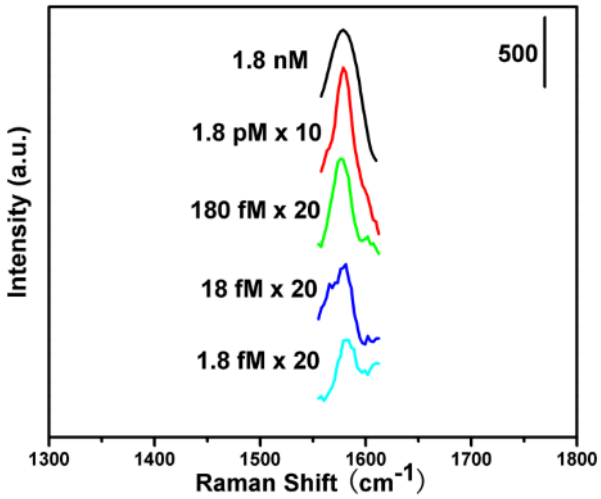

Figure S28. SERS intensity at 1589 cm^{-1} for 4-ATP at different concentrations detected using SLIPSERS.

SUPPLEMENTARY INFORMATION

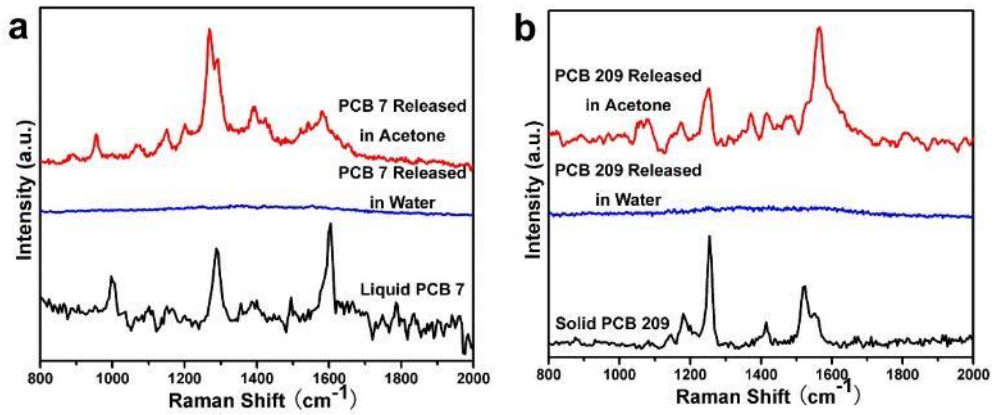

Figure S29. PCB detection from contaminated soil in various solvents. a, PCB 7. **b,** PCB 209.

SUPPLEMENTARY INFORMATION

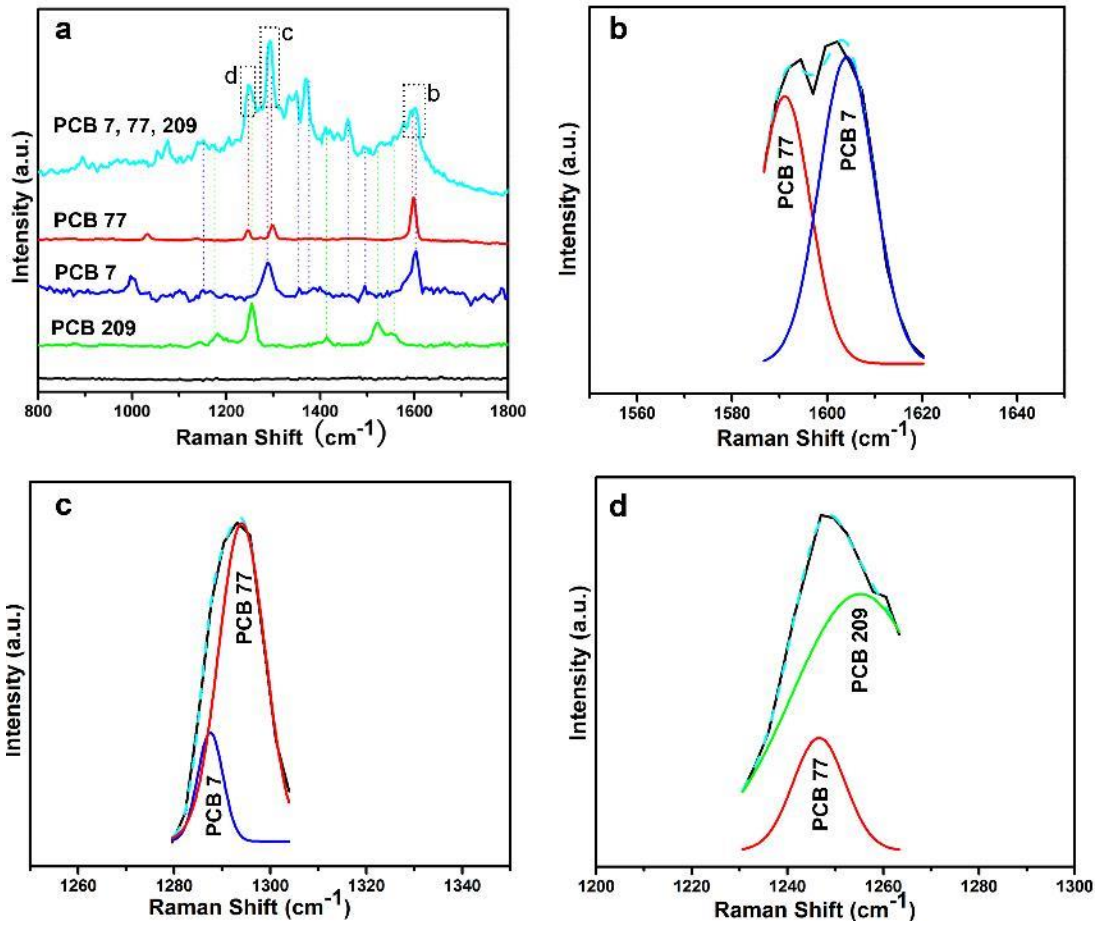

Figure S30. Gaussian deconvolution of the SERS spectrum during multiplex detection of PCBs in contaminated soil. **a,** Multiplex SERS detection of PCB 7, PCB 77, and PCB 209 released from contaminated soil. **b, c,** and **d,** Results of Gaussian deconvolution for the curves indicated in the marked rectangular regions shown in **a**. The dashed cyan line in **b, c,** and **d** are the fitted curves resulting from the summation of individual SERS intensities from PCB 7, PCB 77 and PCB 209.

SUPPLEMENTARY INFORMATION

References

(1) Yang SK, *et al.* (2011) Template-confined dewetting process to surface nanopatterns: fabrication, structural tenability, and structure-related properties. *Adv Funct Mater* 21(13):2446-2455.

(2) Frens G (1973) Controlled nucleation for the regulation of the particle size in monodisperse gold suspensions. *Nature* 241:20-22.

(3) Lyu LM, Wang WC, Huang MH (2010) Synthesis of Ag_2O nanocrystals with systematic shape evolution from cubic to hexapod structures and their surface properties. *Chem Eur J* 16(47):14167-14174.

(4) Fang J, Liu S, Li Z (2011) Polyhedral silver mesocages for single particle surface-enhanced Raman scattering-based biosensor. *Biomaterials* 32(21):4877-4884.

(5) Ivanova EP, et al. (2013) Bactericidal activity of black silicon. *Nature Commun* 4:2838.

(6) Chen X, et al. (2012) Evaporation of droplets on superhydrophobic surfaces: surface roughness and small droplet size effects. *Phys Rev Lett* 109(11):116101.

(7) Yang S, Cai W, Kong L, Lei Y (2010) Surface nanometer-scale patterning in realizing large-scale ordered arrays of metallic nanoshells with well-defined structures and controllable properties. *Adv Funct Mater* 20(15):2527-2533.

(8) Chen B*, et al.* (2014) Green synthesis of large-scale highly ordered core@shell nanoporous Au@Ag nanorod arrays as sensitive and reproducible 3D SERS substrates. *ACS Appl Mater Interfaces* 6(18):15667-15675.

(9) De Angelis F*, et al.* (2011) Breaking the diffusion limit with super-hydrophobic delivery of molecules to plasmonic nanofocusing SERS structures. *Nat Photonics* 5(11):682-687.

(10) Cecchini MP, Turek VA, Paget J, Kornyshev AA, Edel JB (2013) Self-assembled nanoparticle arrays for multiphase trace analyte detection. *Nat Mater* 12(2):165-171.

(11) Wang W, Li Z, Gu B, Zhang Z, Xu H (2009) Ag@SiO2 Core−shell nanoparticles for probing spatial distribution of electromagnetic field enhancement via surface-enhanced Raman scattering. *ACS Nano* 3(11):3493-3496.

(12) Takase M, et al. (2013) Selection-rule breakdown in plasmon-induced electronic excitation of an isolated single-walled carbon nanotube. *Nature Photonics* 7(7):550-554.